Study of models for ray-tracing simulations of thermal neutron monochromators

L. Alianelli[a,b], M. Sánchez del Río[c] and R. Felici[a]

[a] Istituto Nazionale Fisica della Materia, Operative Group in Grenoble
c/o ESRF, BP 220, 38043 Grenoble, France

[b] Institut Laue-Langevin
BP 156, 38042 Grenoble, France

[c]European Synchrotron Radiation Facility
BP 220, 38043 Grenoble, France

ABSTRACT

In recent years there has been a continuous interest in applying ray-tracing techniques for simulating the performance of neutron instruments. This technique is well known for other applications dealing with photon beams (visible, IR, UV and X-rays). Several codes have been developed by different groups to either calculate, with high accuracy, some particular optical elements of a neutron instrument, or to give rough estimations of the whole instrument including simple models of the individual elements. Our goal is to create an optimised code for neutron optics using accurate descriptions for each optical element. In this paper we will analyse the existing models for treating mosaic crystals monochromators. We will report on the calculated and measured diffraction properties of mosaic copper and pyrolytic graphite crystals, which are two of the most commonly used neutron monochromators.

Keywords: Neutron instrumentation; Ray-tracing; Mosaic crystal monochromator.

1. INTRODUCTION

The increasing number of neutron simulation programs recently produced reflects the efforts of the neutron community to push the performance of instruments, which are already in use or are under construction. Some of these codes are programmed for some specific classes of instruments and they allow a precise computation of the response in terms of resolution and intensity: one example is the Restrax program[1] implemented for triple axis spectrometers. On the other side, distributed packages, both Monte Carlo transport and ray-tracing codes, provide a collection of optical elements which can be assembled to simulate any kind of instrument. The Los Alamos code Nisp,[2] with its Web library and interface,[3] has been under development for about 20 years and it provides a collection of optical elements and pre-defined instruments. The Vitess package[4,5] has features which will permit the simulation of instruments at the future European Spallation Source. The McStas code[6,7] is widely used, flexible and well supported.

These packages are often used as black boxes whose output gives the user the response of a complex instrument. It may result difficult to explain the origin of some results and, more important, to address the problem of their reliability. In our opinion, ray-tracing and Monte Carlo methods should be used for accurate computations, otherwise one may consider analytic or graphic approaches. In a simulation including several elements the global accuracy is always less than that of the individual elements. Therefore it is crucial to verify the precision of the description of each optical element before modelling the complete instrument. Our aim is to develop a ray-tracing code based

Other author information: (Send correspondence to L.A.)
L.A.: Email: alianell@ill.fr
Telephone: +33-476 207019; Fax: +33-476 207700

on realistic physical models. For that, two phases are envisaged: i) development of accurate kernels to calculate characteristics of individual elements from first principles (e.g., mosaic crystals, waveguides, supermirrors), and ii) integrate all these kernels in a user friendly environment to allow calculations of the whole instrument.

The starting element in a simulation is the source. It contains all the information on the neutrons at a given starting region: energy, position, direction, probability of presence (or weight). The exact calculation of the emission produced by a reactor or by a spallation source cannot be done analytically. In practice the source characteristics can be input in three ways: 1) From direct measurements of flux. 2) Using data coming from a Monte Carlo particle transport simulation of the reactor core, beam tube and shielding materials (an example is MCNP,[8,9] developed at the Los Alamos National Laboratory and containing cross-sections and physics of neutron transport). 3) Using simple geometrical models, as used in McStas (simple geometrical and energy distribution with an euristical time distribution in the time of flight case) and Vitess (maxwellian distribution from the moderator and pulse shape function of input parameters). A development of a database containing experimental and calculated (e.g. Monte Carlo) sources would be desirable for a ray-tracing simulation.

Among the optical elements, one can distinguish those having a geometrical role (as slits and Sollers) and others having more physical effects requiring a description in terms of reflectivity or transmission: multilayer and supermirror guides, filters, crystal monochromators and analysers. The creation of a database containing the measured response of real optical elements would serve as a base for real reflectivities and a benchmark for ab-initio simulations.

A debated question is the description of those elements which are concerned by the state of polarisation of the beam: Heusler monochromators, magnetic multilayers, polarising filters. The way neutron spin can be tracked in a simulation program dealing with polarised neutron scattering is described by Seeger *et al.*[10] and makes use of the Bloch's equations for the precession of neutron spin in a magnetic field.

The simulation of the scattering properties of the sample are often required, both when calculating the instrument resolution or the flux which is expected to hit the detector: one can simply use an effective source at the sample's place or insert a detailed description of the $S(q, \omega)$ as obtained by calculation or experiment.

The modelling of the detector resolving power and point spread function is often desirable, however these effects can be calculated by post-processing the ideal results produced by ray-tracing.

Our goal is to be able to simulate accurately the complete instrument. We have started looking into the detailed modelling of monochromators. We try to see if current models are well adapted to describe the mosaic crystals monochromators and try to compare the calculations with real data recorded in controlled conditions. We present experimental results, obtained with both X-rays and neutrons, for copper and graphite mosaic crystals and discuss the pros and cons of current models for interpreting the results. From the technical point of view we implemented the physical models in a friendly environment, the software package XOP[11] developed for the X-ray community. Moreover, the inclusion of neutron cross-sections and of source databases in XOP is underway. We will soon release the neutron version of XOP. We will develop in the future a ray-tracing code using the kernels developed here. This code will probably extend the X-ray package SHADOW[12,13] as calculation engine with a user interface adapted from XOP.

2. MODELING THE REFLECTIVITY OF A MOSAIC CRYSTAL

The angular acceptance of a neutron monochromator has to be coupled to the divergence of the incident beam: this can be achieved with the use of non-perfect crystals. The standard neutron monochromator is a mosaic crystal, i.e. a crystals which is considered to be formed by a large number of small perfect crystallites of microscopical or submicroscopical size oriented almost but not exactly, parallel to one another. The drawback is the increased divergence of the beam reflected in the plane of scattering. The discussion on production and performance of crystals with a gradient in the lattice spacing, which would eliminate the disadvantage of the beam widening by mosaic crystals, dates back to the 60's.[14–16] The difficulties in achieving a controlled gradient which give the same reflected

intensity as a mosaic crystal, with a reasonable thickness, has prevented so far the application of gradient crystals. In this paper we will deal with the mosaic deformation. Our work on other kinds of non-perfect crystals will be reported elsewhere.

Mosaic crystals show a much broader diffraction profile as compared to perfect crystals, but with a lower peak reflectivity. The diffraction profiles can be calculated using the theory of Bacon[17] or Zachariasen[18] which are equivalent. They assume that the crystallites are oriented almost parallel to the crystal surface (for Bragg case) following a distribution $W(\theta - \theta_B)$, θ being the angle formed by the incident beam and the Bragg planes and θ_B the Bragg angle. The full-width-at-half-maximum η of this distribution is called mosaic spread or mosaicity. The multiple Bragg reflections in a mosaic crystal and the concept of secondary extinction are summarised by the Darwin equations.[17] An exact and very general solution of these equations has been given by Sears.[19] The physical quantites which govern diffraction by a mosaic crystal are the absorption coefficient μ and the scattering coefficient $\sigma = Q[W(\theta - \theta_B)]$. The Q factor is given by $Q = \lambda^3 F_{hkl}^2 / \left(V_0^2 \sin 2\theta_B\right)$, where λ is the wavelength, F_{hkl} the structure factor and V_0 the unit cell volume. If we define $a = \mu d / \sin\phi$ and $b = \sigma d / \sin\phi$, with d the crystal's thickness and ϕ the angle formed by the incident beam and the surface, the Sears' equations[19] for the reflected and transmitted beam in symmetric Laue (transmission) and Bragg (reflection) geometries are:

$$R_{Laue\,symm} = \frac{1}{2} e^{-a} \left(1 - e^{-2b}\right) \tag{1}$$

$$T_{Laue\,symm} = \frac{1}{2} e^{-a} \left(1 + e^{-2b}\right) \tag{2}$$

$$R_{Bragg\,symm} = \frac{b}{\sqrt{a(a+2b)}\coth\sqrt{a(a+2b)} + (a+b)} \tag{3}$$

$$T_{Bragg\,symm} = \frac{\sqrt{a(a+2b)}}{\sqrt{a(a+2b)}\cosh\sqrt{a(a+2b)} + (a+b)sinh\sqrt{a(a+2b)}} \tag{4}$$

The model is supposed to work if the sample's mosaicity is much larger than the Darwin width of the perfect crystal and if the thickness of the mosaic blocks t_0 is much smaller than the primary extinction depth t_{ext}. According to Zachariasen[18] the correction for primary extinction consists in a smaller scattering factor Q. The actual Q is decreased by a factor $f(A_0)$, where $A_0 \sim t_0/t_{ext}$. Freund *et al.*[20] pointed out that the phenomenon of the complete extinction of the beam in one mosaic block may as well have the effect of a local increase of the absorption cross-section, and that a correction in Q is not sufficient. We will return to this point when presenting the experimental results on pyrolytic graphite.

One consequence of Eqs. 1, 2, 3, 4 is that anomalous absorption is present in Bragg geometry, but not in Laue geometry:

$$[R(\phi) + T(\phi)]_{Laue\,symm} = e^{-\mu d/\sin\phi} \tag{5}$$

$$[R(\phi) + T(\phi)]_{Bragg\,symm} \neq e^{-\mu d/\sin\phi} \tag{6}$$

Both the need for a correct description of the neutron reflectivity of mosaic crystals and the search for new ideas on how to improve the efficiency of neutron monochromators and analysers lead to the problem of determining the cross-sections that mostly contribute to attenuation coefficient μ of the neutron beam. This is the sum of three parts: nuclear absorption, Bragg scattering, and thermal diffuse scattering (TDS):

$$\mu = \frac{n}{V_0}(\sigma_{nucl} + \sigma_{par} + \sigma_{TDS}) \tag{7}$$

where n/V_0 is the number of atoms or molecules per unit cell volume. The TDS cross-section can be calculated as the sum of single phonon and multiple phonon cross-sections: $\sigma_{TDS} = \sigma_{single-ph} + \sigma_{multi-ph}$. There are two main reasons for being interested in TDS cross-sections: i) assessing the behaviour of the total cross-section as a function of temperature and of the incident neutron energy, in order to compute accurately the reflectivity of mosaic crystals, especially at energies greater than the Debye energy of the monochromator crystal; ii) computing, via the knowledge of the differential cross-section, the improved resolution and background of cooled analysers, a solution which has been adopted for the graphite analysers of the TOF spectrometer IRIS[21] at ISIS. The calculation of TDS has been an important task for neutron scatterers since the first years of neutron research.[22] There are different approaches and approximations to this problem[22–25]: all the authors, except for Binder[25] who gives the coherent cross-section for a polycrystal, use the incoherent approximation for the multi-phonon processes, i.e. they disregard all restrictions coming from the momentum conservation and give a non-zero double differential cross-section in all scattering directions. This gives the correct result at energies much higher than the Debye energy. At lower energy the main contribution to σ_{TDS} is the single phonon scattering cross-section $\sigma_{single-ph}$ which can be calculated without approximations. At intermediate energies coherence effects, i.e. interference of scattering from different sites have to be considered, but they amount to a few percent of the total cross-section.[23] We report here the formula given by Freund[26] for the total multi-phonon cross-section:

$$\sigma_{multi-ph} = \sigma_{free} \left\{1 - \exp\left[-C_2 E \left(B_0 + B\left(T\right)\right)\right]\right\} \tag{8}$$

In this equation the C_2 parameter has to be determined experimentally for each material and $B_0 + B\left(T\right)$ is the mean square atomic displacement.

3. EXPERIMENTAL

3.1. INTRODUCTION

Artificial mosaic crystals are produced by means of different fabrication processes. Pyrolytic graphite is a layered structure manufactured by decomposition of a hydrocarbon gas at very high temperature in vacuum: it has been found that its reflectivity is affected by both inhomogeneities of the mosaic structure and primary extinction. Copper mosaic crystals can be obtained by plastic deformation of grown crystals at room or high temperature. Other methods exist for the production of deformed germanium wafers. As the presence of dislocations or other kinds of defects depends on these processes, the diffraction properties will be different and will agree with the theory only partially. In many cases modelling may be improved by considering a layered mosaic structure.[27]

3.2. COPPER

In a preliminary experiment[28] on the hot neutron three axis spectrometer IN1 of ILL we measured the reflectivity of a copper single crystal as a function of temperature in the range 15-285 Kelvin. The goal was to measure both the absorption coefficient μ as a function of temperature and the reflectivity gain at low temperature. The crystal homogeneity had been previously tested on the hard X-ray Laue diffractometer at ILL[29] and its mosaicity amounted to 3'. The thickness was $d = 0.8$ cm. Measurements have been performed at 100 meV ($\lambda = 0.9$ Å) and 250 meV ($\lambda = 0.57$ Å) in Laue geometry. The presence of multiple diffraction did not allow us to reliably measure the absorption coefficient. By using Eqs. 7 and 8 for absorption, one finds that the calculated gain in the peak reflectivity at low temperature of the <220> reflection is about 24% at 100 meV and 35% at 250 meV: we measured about the 18% of the gain at both energies. Fig. 3.2shows the integrated reflectivity vs. temperature fitted with Eq. 1 and using Eq. 7. Only a scale factor as fitting paramenter was used. The fitting procedure gives no reliable results at 250 meV, but shows a good agreement at 100 meV and above 100 Kelvin. One explanation of this behaviour is that the departure from calculated values increases when the parasitic reflections are more important, i.e. at higher energy. This indicates that the use of cooled monochromators for short wavelength neutrons may not give the expected improvement of efficiency. [IN1] Copper: Integrated reflectivity as a function of temperature. The symbols are the measured values and the dotted line is the fit performed above 100 Kelvin.

In this section we will report more extensively on a set of measurements performed on the same sample on the T13 diffractometer at ILL using 48 meV ($\lambda = 1.3$ Å) neutrons. In order to optimize the experiment, we indexed the multiple Bragg reflections using the method described by Cole *et al.*[30] and implemented in XOP. The neutron energy was chosen so that this effect could be minimized by rotating the azimuthal angle of the crystal. We used a perfect crystal Ge <220> monochromator and the beam was collimated to a value of 10'. The sample's reflection and the geometry were the same as in the previous experiment on IN1, i.e. <220> in transmission and the Bragg angle was $\theta_B = 30.57^o$. The angular dependence of both the reflected and transmitted beams were recorded at the following values of temperature: 77, 115.5, 187, 233 and 289 Kelvin.

We fitted $R + T$ by using Eq. 5 in order to retrieve μ, then we fitted R with a lorentzian R_{lor} plus a linear background. The angular dependence of R (after removing the background) and T are plotted in Fig. 1. The fitting results are also reported: the dashed line is $e^{-\mu d/\sin\phi}$; the solid lines are R_{lor} and $(e^{-\mu d/\sin\phi} - R_{lor})$. The fitted μ is reported in Table 1. The error is less than 1% i.e. smaller than the difference with the values calculated by using Eqs. 7 and 8. The fitted μ was used to calculate the theoretical peak reflectivity and this was compared to the peak of R_{lor}. The measured peak reflectivity is 20% smaller than expected. The beam divergence is probably one of the reasons for observing a lower reflectivity. However the attempt to fit R with Eq. 1 and taking into account the beam divergence (by convoluting the theoretical reflectivity curve with the incident beam shape) did not succeed: in our opinion this is due to the non-ideal mosaic structure. A lower peak reflectivity has been observed also with high energy X-rays on a sample produced with the same technique and analysed at the ID15 beamline of the ESRF. The measured and calculated peak values for the <002>, <004>, and <006> reflections in symmetric Bragg geometry at X-ray energy of 96 keV ($\lambda = 0.13$ Å) and 136 keV ($\lambda = 0.09$ Å) are reported in Table 2: the difference is always more than 50% . Concerning this experiment, it is worth mentioning that we also recorded some diffraction topographs which showed the presence of structures or grains. Moreover the high energy X-ray rocking curves were asymmetrical and had a double peak structure in some cases.

Table 1. Neutron absorption and peak reflectivity for the copper sample at 48 meV. The reflection used is the <220> in symmetric Laue geometry. Freund's[26] formulas and C_2 parameter have been used for calculating μ.

Temperature Kelvin	μ_{calc} cm^{-1}	μ_{fit} cm^{-1}	$R_{peak-calc}$	$R_{peak-meas}$
77	0.307	0.2735	0.388	0.317
115.5	0.3275	0.306	0.376	0.302
187.3	0.368	0.345	0.363	0.289
232.8	0.3935	0.366	0.356	0.279
288.9	0.424	0.396	0.346	0.271

Table 2. High energy X-ray reflectivity of a copper sample of mosaicity $\eta = 5'$.

Energy keV	Reflection	Measured peak reflectivity	Calculated peak reflectivity
96	<200>	0.095	0.294
96	<400>	0.0245	0.089
96	<600>	0.0084	0.0302
136	<200>	0.123	0.288
136	<400>	0.027	0.086
136	<600>	0.009	0.029

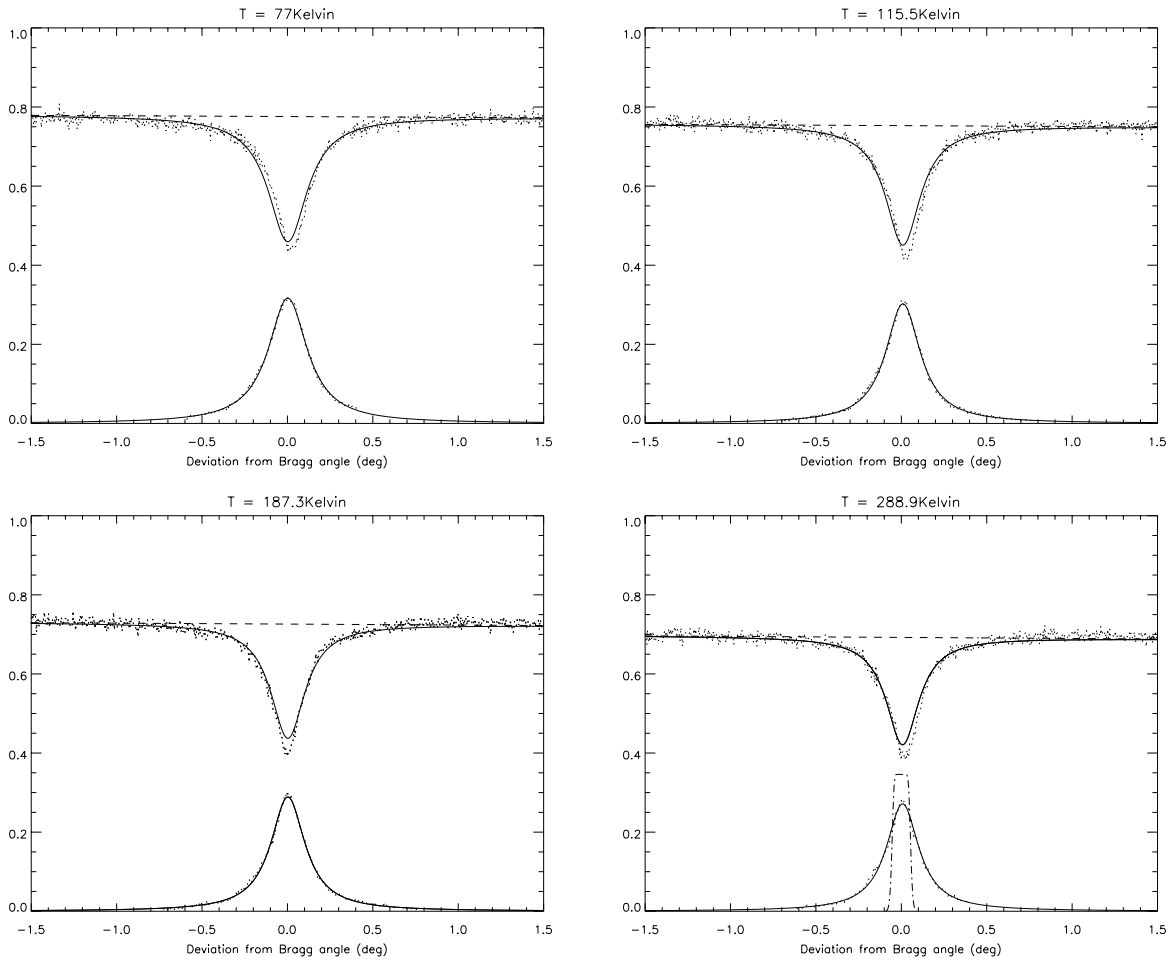

Figure 1. Copper at 48 meV, <220> reflection in Laue geometry. Angular dependence of the normalised transmitted and reflected beams for different values of temperature. The dotted lines are the measured T and R. The dashed line is the fit of $R + T = e^{-\mu d/\sin\phi}$. The solid lines are the fit: R_{lor} and $(e^{-\mu d/\sin\phi} - R_{lor})$. The dashed-dotted line in the last figure is the theoretical reflectivity for a mosaicity of 3' (FWHM).

3.3. GRAPHITE

Pyrolytic graphite is generally considered as a nearly ideal imperfect crystal. Extensive studies of its diffracting properties have been done in the past[20,31] but, to our knowledge, a complete analysis of its reflectivity as a function of energy and index of reflection does not exist. We performed measurements of reflection and transmission curves using synchrotron radiation at the BM5 beamline at ESRF. The source was a bending magnet with a critical energy of 20 keV. The beamline was equipped with a flat double crystal Si <111> monochromator (giving an energy resolution of about $\delta E/E \sim 10^{-4}$) placed at 30 m from the source. The sample was mounted at 40 m from the source on a 3-axes diffractometer using the horizontal plane as diffracting plane. The divergence of the beam in the scattering plane could be considered practically zero and its dimensions were fixed to $0.1mm \times 0.1mm$. The curves were measured using a Si diode detector. We used a sample of thickness $d = 0.5$ mm produced by Optigraph (Russia) and measured the <002> and <004> reflections in Bragg symmetric geometry at 12, 22, 32 and 42 keV (λ=1.03, 0.56, 0.39 and 0.295 Å). We tested the sample's homogeneity by recording diffraction topographs at all reflection and energies mentioned above. First the absorption coefficient μ was obtained by fitting the tails of T, then these values were used to fit the rocking and transmission curves simultaneously with Eqs. 3 and 4. The fitting parameters were mosaicity η and the scattering factor Q. The results are shown in Fig 2. The fit performed on the tails of T is good

(thus giving reliable values for the absorption coefficient) except for the case of the <002> reflection at $E \geq 22keV$: one possible reason for the non accurate fit may be that in these cases the Bragg angles are quite small (see Table 3) and the presence of possible defects or inhomogeneities on the surface affects the beam. The fit of the rocking curves, on the other hand, is very accurate for the <004> reflection but not for the <002>: the fitted peak reflectivity of the principal reflection is always smaller than the measured one. Table 3 summarizes the fit results. The value of mosaicity, as obtained by the fit, was equal to $\eta = 0.32^o$.

Table 3. Parameters of the pyrolytic graphite sample: Bragg angles, X-ray absorption coefficient and Q factor.

Energy keV	Reflection	θ_{Bragg} degrees	μ_{calc} cm^{-1}	μ_{fit} cm^{-1}	Q_{calc} cm^{-1}	Q_{fit} cm^{-1}
12	<002>	8.88	2.84	2.31	0.0638	0.0470
12	<004>	18.	2.84	2.31	0.00809	0.00584
22	<002>	4.83	0.73	0.61	0.0211	0.0163
22	<004>	9.69	0.73	0.67	0.00314	0.00227
32	<002>	3.32	0.49	0.29	0.00963	0.0061
32	<004>	6.65	0.49	0.44	0.00156	0.00116
42	<002>	2.53	0.425	0.16	0.005615	0.00265
42	<004>	5.06	0.425	0.32	0.00926	0.0007

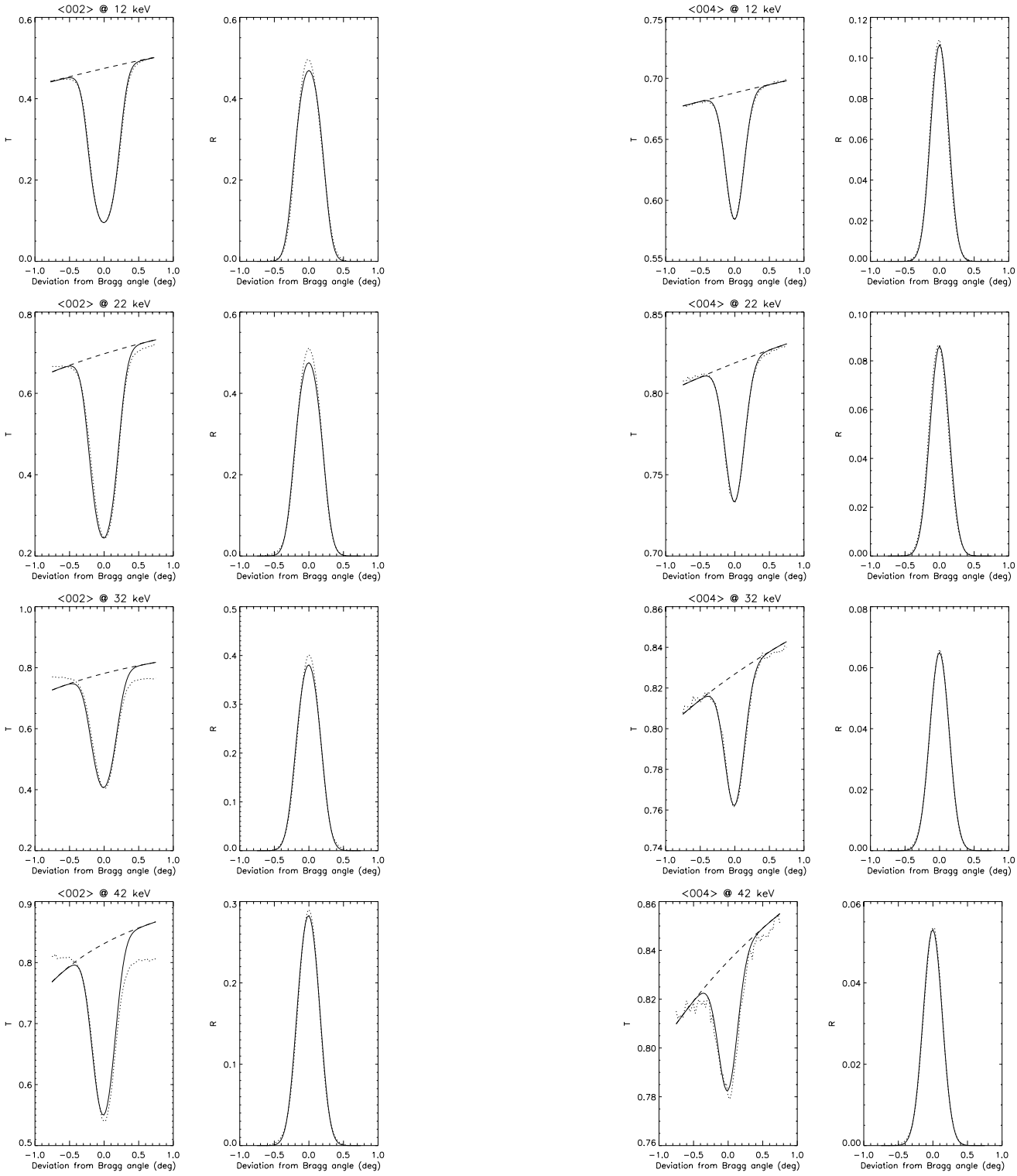

Figure 2. Graphite: normalised transmission and reflectivity as a function of the X-ray energy for the <002> and <004> reflections. The dotted line is the experiment. The absorption coefficient was obtained by fitting the tails of the experimental T (dashed line), then R and T were fitted simultaneously in order to retrieve the Q factor and mosaicity η. The solid lines are the fit.

4. SUMMARY AND CONCLUSIONS

In the case of graphite we succeeded in performing good fits, thus retrieving the physical parameters μ, η and Q, in the following cases: <002> reflection at 12 keV and <004> at 12, 22, 32, 42 keV. The fitted absorption coefficient is always smaller than the values calculated by summing photo-electric absorption and Compton scattering. The correction to the Q factor coming from primary extinction in the mosaic blocks is approximately 0.74, giving a block dimension of the same order of magnitude as the primary extinction length. One result concerning this graphite sample (whose homogeneity had been tested by means of X-ray diffraction topography during the same experiment) is that the theory works for the <004> reflection, but in the case of the principal reflection the peak of R is not adequately fitted. Moreover, only a correction in Q seems necessary when accounting for primary extinction effects.

We performed neutron and high energy X-ray measurements on two copper samples produced with the same technique: in both cases the fitting of the reflectivity curves with the theoretical formulas was not successful. However, we measured the neutron absorption coefficient at 48 meV as a function of temperature with a good accuracy. We will repeat the measurements with other materials commonly used as monochromators in order to have a database of real cross-sections and reflectivity values. The synchrotron experiments on copper confirm that the reflectivity is less than expected and this is probably due to the presence of structures. We will carry on the same kind of measurements on other materials (e.g. germanium) in order to have a more complete idea of the reflectivity of artificial mosaic crystals.

ACKNOWLEDGEMENTS

We wish to thank the ILL and the ESRF for access to their facilities. We acknowledge A. Ivanov and I. Anderson for many explanations on the neutron experiments and for reading the paper. We are very grateful to P. Courtois and B. Hamelin for access to the T13 instrument and for providing the copper sample and to E. Hetzler and R. Hehn for technical assistance. Thanks also to M. Gambaccini, P. Baldelli, C. Pellicciari and A. Taibi for lending us the graphite sample and for help during the experiment at BM5 and to G. Pareschi for helpful discussions.

REFERENCES

1. J. Saroun and J. Kulda, "RESTRAX - a program for TAS resolution calculation and scan profile simulation", *Physica B: Condensed Matter* **234-236**, pp. 1102-1104, 1997.
2. P.A. Seeger, L.L. Daemen, T.G. Thelliez and R.P. Hjelm, "Neutron instrument simulations in the next millennium", *Physica B: Condensed Matter* **283**, pp. 433-435, 2000.
3. http://strider.lansce.lanl.gov/NISP/Welcome.html
4. D. Wechsler, G. Zsigmond, F. Streffer, J.A. Stride and F. Mezei, "Monte-Carlo simulations for instrumentation at pulsed and continuous sources", *Physica B: Condensed Matter* **276-278**, pp. 71-71, 2000.
5. http://www.hmi.de/projects/ess/vitess/
6. K. Nielsen and K. Lefmann, "Monte Carlo simulations of neutron-scattering instruments using McStas", *Physica B: Condensed Matter* **283**, pp. 426-432, 2000.
7. http://neutron.risoe.dk/mcstas/
8. J.F. Briesmeister, "MCNP – A General Monte Carlo N-Particle Transport Code", *Los Alamos National Laboratory report LA-13709-M*, 2000.
9. http://www-xdiv.lanl.gov/XCI/PROJECTS/MCNP/
10. P.A. Seeger and L.L. Daemen, "Numerical solution of Bloch's equation for neutron spin precession", *Nucl. Instr. and Meth.* **A457**, pp. 338-346, 2001.
11. M. Sánchez del Río and R.J. Dejus, "XOP: Recent developments", *SPIE proceedings* **3448**, pp. 340-345, 1998.
12. C. Welnak, G.J. Chen and F. Cerrina, "SHADOW: a synchrotron radiation and x-ray optics simulation tool", *Rev. Sci. Instrum.* **A347**, pp. 344-347, 1994.
13. http://www.nanotech.wisc.edu/shadow/shadow.html

14. H. Maier-Leibnitz, "Einige Vorschläge für die Verwndung von Zusammengesetzten Monochroamtorkristallen für Neutronenbeugungs und Streumessungen", *Ann. Acad. Sci. Fenncae, Phys. VI* **267**, pp. 2-17, 1967.
15. B. Alefeld, "Ein perfekter Kristall mit Temperaturgradient als Neutronenmonochromator", *Z. Physik* **228**, pp. 454-464, 1969.
16. G. Albertini, A. Boeuf, G. Cesini, S. Mazkedian, S. Melone and F. Rustichelli, "A simple model for dynamical neutron diffraction by deformed crystals", *Acta Cryst.* **A32**, pp. 863-868, 1976.
17. G.E. Bacon and R.D. Lowde , "Secondary Extinction and Neutron Crystallography", *Acta Cryst.* **1**, pp. 303-314, 1948.
18. W.H. Zachariasen, "Theory of X-ray Diffraction in Crystals", *Dover, New York*, 1945.
19. V.F. Sears, "Bragg Reflection in Mosaic Crystals. I. General solution of the Darwin Equations", *Acta Cryst.* **A53**, pp. 35-45, 1997.
20. A.K. Freund, A. Munkholm and S. Brennan, "X-Ray Diffraction Properties of Highly Oriented Pyrolytic Graphite", *SPIE proceedings* **2856**, pp. 68-79, 1996.
21. C.J. Carlile, M.A. Adams, P.S.N. Krishna, M. Prager, K. Shibata, P. Westerhuijs, "Less background, better contrast by cooling analyser crystals", *Nucl. Instr. and Meth.* **A338**, pp. 78-82, 1994.
22. G. Placzek, "The scattering of Neutron by Systems of Heavy Nuclei", *Phys. Rev.* **86**, pp. 377-388, 1952.
23. W. Marshall and S.W. Lovesey, "Theory of thermal neutron scattering", *Clarendon Press, Oxford*, 1971.
24. V.F. Turchin , "Slow neutrons", *Israel Program for Scientific Translations*, 1965.
25. K. Binder, "Total Coherent Cross Sections for the Scattering of Neutrons from Crystals", *Phys. Stat. Sol.* **41**, pp. 767-779, 1970.
26. A.K. Freund, "Cross-sections of materials used as neutron monochromators and filters", *Nucl. Instr. and Meth.* **213**, pp. 495-501, 1983.
27. B. Dorner, "Measurements of absolute reflectivities of mosaic crystals and their wavelength dependence", *J. Appl. Cryst.* **4**, pp. 185-190, 1971.
28. L. Alianelli, M. Sánchez del Río, A. Ivanov, B. Hamelin, R. Felici, I. Anderson, "Reflectivity test at low temperature on a mosaic copper crystal", *ILL Experimental Report*, TEST $N°464$, 2000.
29. P. Bastie and B. Hamelin, "La méthode de Laue refocalisée à haute énergie: une technique d'étude en volume des monocristaux ", *Journal de Physique IV* **6**, pp. C4/13-C4/21, 1996.
30. H. Cole, F.W. Chambers and H.M. Dunn, "Simultaneous Diffraction: Indexing Umweganregung Peaks in Simple Cases", *Acta Cryst.* **15**, pp. 138-144, 1962.
31. A. Tuffanelli, M. Sánchez del Río, G. Pareschi, M. Gambaccini, A. Taibi, A. Fantini and M. Ohler, "A comparative characterization of Highly Oriented Pyrolytic Graphite by means of diffraction topography", *SPIE proceedings* **3773**, pp. 192-198, 1999.